Polarized focused vortex beams: half-order phase vortices

Colin J. R. Sheppard*

Istituto Italiano di Tecnologia, Genova 16163, Italy
*colinjrsheppard@gmail.com

Abstract: A theoretical treatment is presented for the focusing of polarized vortex beams, including the generation of Bessel beams. A combination of a phase vortex with arbitrary topological charge, and a polarization vortex of arbitrary order is considered. Results are given for both paraxial and high NA systems. Conditions for the presence of non-zero on-axis intensity are given. An interesting observation is that half-order phase vortices can exist, without the existence of any phase discontinuity. The behavior of Bessel beams with half-order phase vortices is investigated.

OCIS codes: (050.1960) Diffraction theory; (050.4865) Optical vortices; (260.1960) Diffraction theory; (260.2110) Electromagnetic optics; (260.5430) Polarization.

References and links

1. J. F. Nye and M. Berry, "Dislocations of wave-fronts," Proc. R. Soc. Lond. A Math. Phys. Sci. **336**(1605), 165–190 (1974).
2. W. J. Condell, "Fraunhoffer diffraction from a circular aperture with helical phase factor," J. Opt. Soc. Am. **2**(2), 206 (1985).
3. V. Y. Bazhenov, M. S. Soskin, and M. V. Vasnetsov, "Screw dislocations in light wave-fronts," J. Mod. Opt. **39**, 985–990 (1992).
4. N. Heckenberg, R. McDuff, C. P. Smith, and H. Rubinstein Dunlop, "Laser beams with phase singularities," Opt. Quantum Electron. **24**, S951–S962 (1992).
5. V. V. Kotlyar and V. A. Soifer, "Rotor spatial filter for analysis and synthesis of coherent fields," Opt. Commun. **89**(2–4), 159–163 (1992).
6. G. Indebetouw, "Optical vortices and their applications," J. Mod. Opt. **40**(1), 73–87 (1993).
7. I. Freund, N. Shvartsman, and V. Freilikher, "Optical dislocation networks in highly random media," Opt. Commun. **101**(3–4), 247–264 (1993).
8. M. Totzeck and H. J. Tiziani, "Phase-singularities in 2D diffraction fields and interference microscopy," Opt. Commun. **138**(4–6), 365–382 (1997).
9. L. W. Davis and G. Patsakos, "TM and TE electromagnetic beams in free space," Opt. Lett. **6**(1), 22–23 (1981).
10. G. P. Agrawal and M. Lax, "Free-space wave propagation beyond the paraxial approximation," Phys. Rev. A **27**(3), 1693–1695 (1983).
11. R. Simon, E. C. G. Sudarshan, and N. Mukunda, "Gaussian-Maxwell beams," J. Opt. Soc. Am. A **3**(4), 536–540 (1986).
12. R. H. Jordan and D. G. Hall, "Free-space azimuthal paraxial wave equation: the azimuthal Bessel-Gauss beam solution," Opt. Lett. **19**(7), 427–429 (1994).
13. Z. Bouchal and M. Olivík, "Non-diffractive vector Bessel beams," J. Mod. Opt. **42**(8), 1555–1566 (1995).
14. D. G. Hall, "Vector-beam solutions of Maxwell's wave equation," Opt. Lett. **21**(1), 9–11 (1996).
15. P. L. Greene and D. G. Hall, "Diffraction characteristics of the azimuthal Bessel-gauss beam," J. Opt. Soc. Am. A **13**(5), 962–966 (1996).
16. P. L. Greene and D. G. Hall, "Properties and diffraction of the azimuthal Bessel-Gauss beam," J. Opt. Soc. Am. A **15**(12), 3020–3027 (1998).
17. C. J. R. Sheppard and S. Saghafi, "Transverse-electric and transverse-magnetic beam modes beyond the paraxial approximation," Opt. Lett. **24**(22), 1543–1545 (1999).
18. S. Quabis, R. Dorn, M. Eberler, O. Glockl, and G. Leuchs, "Focusing light to a tighter spot," Opt. Commun. **179**(1–6), 1–7 (2000).
19. K. S. Youngworth and T. G. Brown, "Focusing of high numerical aperture cylindrical-vector beams," Opt. Express **7**(2), 77–87 (2000).
20. S. Quabis, R. Dorn, M. Eberler, O. Glockl, and G. Leuchs, "The focus of light - theoretical calculation and experimental tomographic reconstruction," Appl. Phys. B **72**(1), 109–113 (2001).
21. L. E. Helseth, "Optical vortices in focal regions," Opt. Commun. **229**(1–6), 85–91 (2004).
22. C. J. R. Sheppard, N. K. Balla, S. Rehman, E. Y. S. Yew, and W. T. Teng, "Bessel beams with the tightest focus," Opt. Commun. **282**, 4647–4656 (2009).

#212728 - $15.00 USD Received 26 May 2014; revised 10 Jul 2014; accepted 11 Jul 2014; published 18 Jul 2014

23. X. Hao, C. F. Kuang, T. T. Wang, and X. Liu, "Phase encoding for sharper focus of the azimuthally polarized beam," Opt. Lett. **35**(23), 3928–3930 (2010).
24. C. J. R. Sheppard and S. Rehman, "Highly convergent focusing of light based on rotating dipole polarization," Appl. Opt. **50**(22), 4463–4467 (2011).
25. J. F. Nye, "Polarization effects in the diffraction of electromagnetic waves: the role of disclinations," Proc. R. Soc. Lond. A Math. Phys. Sci. **387**(1792), 105–132 (1983).
26. J. F. Nye, "Lines of circular polarization in electromagnetic wave fields," Proc. R. Soc. Lond. A Math. Phys. Sci. **389**(1797), 279–290 (1983).
27. J. F. Nye and J. V. Hajnal, "The wave structure of monochromatic electromagnetic waves," Proc. R. Soc. Lond. A Math. Phys. Sci. **409**(1836), 21–36 (1987).
28. J. V. Hajnal, "Singularities in the transverse fields of electromagnetic waves, 1. Theory," Proc. R. Soc. Lond. A Math. Phys. Sci. **414**(1847), 433–446 (1987).
29. J. V. Hajnal, "Singularities in the transverse fields of electromagnetic waves, 2. Observations on the electric field," Proc. R. Soc. Lond. A Math. Phys. Sci. **414**(1847), 447–468 (1987).
30. J. F. Nye, *Natural Focusing and Fine Structure of Light* (Institute of Physics Publishing, 1999).
31. C. J. R. Sheppard, "Polarization of almost-plane waves," J. Opt. Soc. Am. A **17**(2), 335–341 (2000).
32. J. Lekner, "Polarization of tightly focused laser beams," J. Opt. A, Pure Appl. Opt. **5**(1), 6–14 (2003).
33. B. Richards and E. Wolf, "Electromagnetic diffraction in optical systems. II Structure of the image field in an aplanatic system," Proc. R. Soc. Lond. A Math. Phys. Sci. **253**(1274), 358–379 (1959).
34. X. S. Xie and R. C. Dunn, "Probing single molecule dynamics," Science **265**(5170), 361–364 (1994).
35. W. P. Ambrose, P. M. Goodwin, R. A. Keller, and J. C. Martin, "Alterations of single molecule fluorescence lifetimes in near-field optical microscopy," Science **265**(5170), 364–367 (1994).
36. A. Drechsler, M. A. Lieb, C. Debus, A. J. Meixner, and G. Tarrach, "Confocal microscopy with a high numerical aperture parabolic mirror," Opt. Express **9**(12), 637–644 (2001).
37. M. A. Lieb and A. J. Meixner, "A high numerical aperture parabolic mirror as imaging device for confocal microscopy," Opt. Express **8**(7), 458–474 (2001).
38. N. Huse, A. Schönle, and S. W. Hell, "Z-polarized confocal microscopy," J. Biomed. Opt. **6**(3), 273–276 (2001).
39. H. He, M. E. J. Friese, N. R. Heckenberg, and H. Rubinsztein-Dunlop, "Direct observation of transfer of angular momentum to absorptive particles from a laser beam with a phase singularity," Phys. Rev. Lett. **75**(5), 826–829 (1995).
40. M. E. J. Friese, T. A. Nieminen, N. R. Heckenberg, and H. Rubinsztein-Dunlop, "Optical alignment and spinning of laser-trapped microscopic particles," Nature **394**(6691), 348–350 (1998).
41. X. Hao, C. F. Kuang, T. T. Wang, and X. Liu, "Effects of polarization on the de-excitation dark focal spot in STED microscopy," J. Opt. **12**(11), 115707 (2010).
42. S. Galiani, B. Harke, G. Vicidomini, G. Lignani, F. Benfenati, A. Diaspro, and P. Bianchini, "Strategies to maximize the performance of a STED microscope," Opt. Express **20**(7), 7362–7374 (2012).
43. C. J. R. Sheppard, "Polarization of beams and highly focused waves," in *ICO Topical Meeting on Polarization Optics*, Polvijärvi, Finland (2003).
44. W. T. Tang, E. Y. Yew, and C. J. Sheppard, "Polarization conversion in confocal microscopy with radially polarized illumination," Opt. Lett. **34**(14), 2147–2149 (2009).
45. P. Török, P. Varga, Z. Laczik, and G. R. Booker, "Electromagnetic diffraction of light focused through a planar interface between materials of mismatched refractive indices: an integral representation," J. Opt. Soc. Am. A **12**(2), 325–332 (1995).
46. C. Zhao and J. H. Burge, "Orthonormal vector polynomials in a unit circle, Part I: basis set derived from gradients of Zernike polynomials," Opt. Express **15**(26), 18014–18024 (2007).
47. C. Zhao and J. H. Burge, "Orthonormal vector polynomials in a unit circle, Part II : completing the basis set," Opt. Express **16**(9), 6586–6591 (2008).
48. C. J. R. Sheppard, "Electromagnetic field in the focal region of wide-angular annular lens and mirror systems," IEE J. Microwaves Opt. Acoust. **2**, 163–166 (1978).
49. D. Fink, "Polarization effects of axicons," Appl. Opt. **18**(5), 581–582 (1979).
50. I. V. Basistiy, V. A. Pas'ko, V. V. Slyusar, M. S. Soskin, and M. V. Vasnetsov, "Synthesis and analysis of optical vortices with fractional topological charges," J. Opt. A, Pure Appl. Opt. **6**(5), S166–S169 (2004).
51. V. V. Kotlyar, A. A. Almazov, S. N. Khonina, V. A. Soifer, H. Elfstrom, and J. Turunen, "Generation of phase singularity through diffracting a plane or Gaussian beam by a spiral phase plate," J. Opt. Soc. Am. A **22**(5), 849–861 (2005).
52. K. G. Larkin, D. J. Bone, and M. A. Oldfield, "Natural demodulation of two-dimensional fringe patterns. I. General background of the spiral phase quadrature transform," J. Opt. Soc. Am. A **18**(8), 1862–1870 (2001).
53. K. G. Larkin, "Natural demodulation of two-dimensional fringe patterns. II. Stationary phase analysis of the spiral phase quadrature transform," J. Opt. Soc. Am. A **18**(8), 1871–1881 (2001).
54. C. J. R. Sheppard and T. Wilson, "Gaussian-beam theory of lenses with annular aperture," IEE J. Microwaves Opt. Acoust. **2**, 105–112 (1978).
55. J. Durnin, J. J. Miceli, Jr., and J. H. Eberly, "Diffraction-free beams," Phys. Rev. Lett. **58**(15), 1499–1501 (1987).

#212728 - $15.00 USD Received 26 May 2014; revised 10 Jul 2014; accepted 11 Jul 2014; published 18 Jul 2014

1. Introduction

At present, there continues to be strong interest in the properties of phase vortices [1–8], and also polarization vortices [9–24]. At a phase vortex, at the centre of which the electric field is zero, the phase changes by an integer (called the topological charge) multiplied by 2π radians on travelling around the singularity. It carries orbital angular momentum of integer charge. A polarization vortex is defined as a structure including a point where the transverse electric field is zero, and the polarization state therefore undefined. A particular example of polarization vortex is when the field is inhomogeneous and locally plane-polarized, the direction of the field rotating by an integer (called the order) multiplied by 2π radians on travelling around the singularity. The polarization vortex carries no angular momentum, but on travelling around the singularity the geometric (Pancharatnam) phase changes by an integral number of 2π radians.

Note that the polarization vortex considered here, with a zero in electric field, is different from the generic polarization singularities naturally present in optical fields [25–30]. Nye has pointed out that in generic fields there are no points where the electric field is zero at all times [30]. However, here we are concerned with engineering the presence of these polarization vortices. Nye describes polarization singularities such as lines of circular polarization, surfaces of linear polarization, and disclinations in instantaneous field distributions. Although these singularities are different from the polarization vortices, there are some topological similarities.

Some general properties of the polarization of almost-plane waves have been described [31]. General properties of the polarization of tightly focused beams have also been discussed by Lekner [32].

Focusing of waves exhibiting phase vortices has been investigated by Condell, and Kotlyar and Soifer [2, 5]. However, their treatment was limited to paraxial optics. Similarly, paraxial treatments of polarization vortices have been presented [12, 14–16]. Propagation properties of non-paraxial beams with polarization vortices have also been described [9–11, 17]. There is great interest currently in the focusing of waves with lenses of high numerical aperture (NA), such as a microscope objective. The important case of focusing of a linearly polarized wave was analysed by Richards and Wolf [33]. More recently, focusing of waves of other polarization distributions has been reported [13, 18–20]. One reason for this interest is the possibility of producing a more highly localized focal distribution in this way. Another reason is that the orientation of a fluorescent molecule can be determined by illumination by a wave of appropriate polarization, as in single-molecule fluorescence studies [34–38]. A third application is in optical trapping of absorbing particles, or particles with refractive index lower than the surroundings, and in rotation of these particles [39, 40]. A fourth application is the generation of doughnut beams for STED (stimulated emission depletion microscopy) [41, 42].

Here, we combine these two areas, and investigate the focusing of waves with various phase and polarization properties by a high numerical aperture lens, concentrating in particular on Bessel beams. Although Bessel beams are a specific example, they can be integrated up to produce more general beams or simulate a lens aperture. Although there is much in common between the two types of vortex, few papers seem to have considered the combination. We presented a preliminary study [43]: one important observation is that a tightly focused azimuthally polarized beam with a unity charge phase singularity gives a non-zero field on the axis, coupled with a small focal spot [21–24]. Helseth considered the combination of azimuthally or radially polarized beams with phase singularities, and showed that radial polarization with a unity charge phase singularity gives a non-zero field on-axis, even for paraxial focusing [21]. This effect has been exploited to focus paraxially radially-polarized light to a spot [44]. However, to our knowledge no paper has analyzed the behavior of a combination of a phase vortex of arbitrary charge with a polarization vortex of arbitrary order. Polarization vortices of order two, in particular, are very common in focusing systems.

#212728 - $15.00 USD Received 26 May 2014; revised 10 Jul 2014; accepted 11 Jul 2014; published 18 Jul 2014

For example, high NA focusing of a plane wave gives a component with a polarization vortex of order two in the focal region [31].

2. Phase and polarization of an almost plane wave

As an electromagnetic wave must satisfy Maxwell's equations, it follows that any wave that is not of infinite extent must include a z component of either electric or magnetic field, and cannot be purely plane polarized. However, if the variation in the amplitude of the wave is slowly varying relative to the wavelength, we can assume that the amplitude and polarization state varies in an arbitrary way over the wavefront, and that the z components of field are negligible. For the case of focusing by a lens of high numerical aperture in the Debye approximation, the incident waveform can be assumed to be polarized on the Gaussian reference sphere, equivalent to the strength of an angular spectrum of plane waves. Further, the strength and polarization of the angular spectrum of plane waves can be calculated from the incident fields by the vectorial method of Richards and Wolf, or the matrix method of Török *et al.* [33, 45]. The amplitude in the front focal plane of the lens can be assumed to be an almost-plane wave, over the entrance pupil. Here, we are concerned with locally linearly polarized illumination for a few modes of low order, but more general behavior has been considered elsewhere [31]. In a different context, we also note research on vector Zernike polynomials [46, 47].

We consider combinations of polarization and phase vortices as circular harmonics, so that we can write for the locally linearly-polarized electric field in the front focal plane of the lens $\mathbf{E}_{1,2}$

$$\begin{aligned} \mathbf{E}_1 &= \rho^{|m|+|n|}\left(\cos m\phi\,\mathbf{i} + \sin m\phi\,\mathbf{j}\right)\exp\left(in\phi\right), \\ \mathbf{E}_2 &= \rho^{|m|+|n|}\left(-\sin m\phi\,\mathbf{i} + \cos m\phi\,\mathbf{j}\right)\exp\left(in\phi\right), \end{aligned} \tag{1}$$

where m, n are integers, being the order of the polarization vortex and charge of the phase vortex, respectively, ρ,ϕ are cylindrical coordinates, and $\mathbf{i},\mathbf{j}$ are unit vectors in the Cartesian x,y directions. The electric field is locally linearly polarized, but with spatially varying orientation. Then $m=0$ corresponds to x or y polarized, respectively for solutions 1 and 2. In cylindrical coordinates these become

$$\begin{aligned} \mathbf{E}_1 &= \rho^{|m|+|n|}\left\{\cos[(m-1)\phi]\mathbf{a}_\rho + \sin[(m-1)\phi]\mathbf{a}_\phi\right\}\exp\left(in\phi\right), \\ \mathbf{E}_2 &= \rho^{|m|+|n|}\left\{-\sin[(m-1)\phi]\mathbf{a}_\rho + \cos[(m-1)\phi]\mathbf{a}_\phi\right\}\exp\left(in\phi\right), \end{aligned} \tag{2}$$

where $\mathbf{a}_\rho,\mathbf{a}_\phi$ are unit vectors in the ρ,ϕ directions. We see that $m=1$ corresponds to radial (also called TM_{01}) and azimuthal polarization (also called TE_{01}), respectively, both corresponding to an antiparallel screw disclination [25, 31]. The cases when $m=-1$ correspond to a parallel screw disclination, or saddle, (TE_{21} or TM_{21}). Another important case is the polarization vortex of order two ($m=2$), or dipole, which can be generated on grazing incidence reflection from a deep paraboloid (or toroidal) mirror [48], or reflective axicon (waxicon) [49]. The input polarizations for different values of m , for $n=0$, are illustrated in Fig. 1 for the first (upper) case.

Interestingly, the form in Eqs. (1), (2) is valid even for non-integer values of *m* and *n*. The cases (1/2, 1/2) and (–1/2,1/2) are particular cases where the polarization of the electric field rotates by π radians on circling around the origin, but the direction of the electric field matches up after a complete rotation because of the phase introduced by the phase dislocation, as shown in the time sequences in Fig. 2(a) (Media 1) and Fig. 2(b) (Media 2). These correspond topologically to the so-called lemon and star singularities [25]. For Fig. 1, on the other hand, $n=0$ and so there is a discontinuity in polarization for non-integer values of m . Other papers have considered fractional topological charge, but for a scalar system this

#212728 - $15.00 USD Received 26 May 2014; revised 10 Jul 2014; accepted 11 Jul 2014; published 18 Jul 2014

necessarily results in a phase discontinuity [50]. The three-fold symmetry for $m=-1/2$ in Fig. 1 and Fig. 2(b) is apparent from Eq. (2).

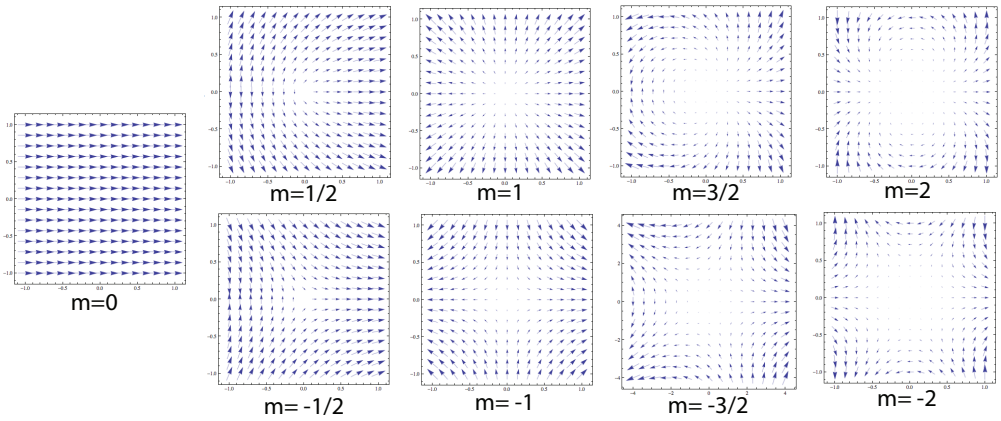

Fig. 1. The input field polarizations (inhomogeneous, locally linear polarization) for different values of m, for $n=0$, for the first (upper) case of Eq. (1). The arrow length is proportional to the field strength.

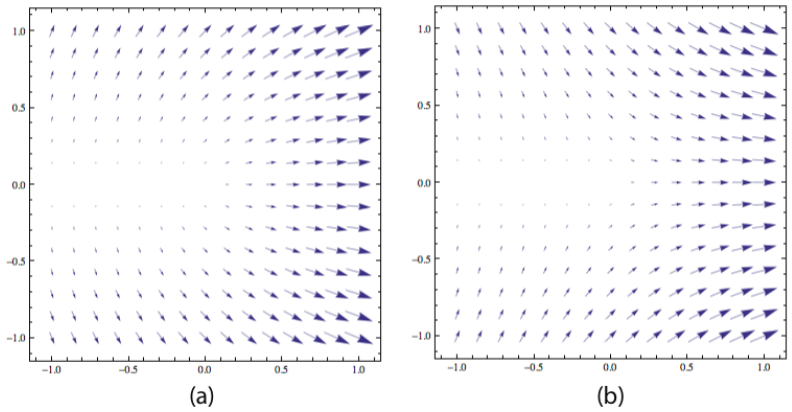

Fig. 2. Input vector field at time $t=0$, with the time variation shown in the Media, for (a) $m=1/2, n=1/2$ (Media 1), (b) $m=-1/2, n=1/2$ (Media 2).

As the amplitude of the wave can be altered, as desired, using a mask [51], we take the power of ρ to be more generally g. Indeed, if the polarization or phase of an initially plane-polarized wave is modified using a spatial light modulator, then $g=0$ as the intensity of the wave is not changed. The particular case when $g=0$ and $n=1$ is very interesting, as it has been shown to exhibit properties expected of a two-dimensional Hilbert transform [52, 53].

Equation (1) can be written

$$\begin{aligned}\mathbf{E}_1 &= \frac{1}{2}\rho^g\left\{(\mathbf{i}-i\,\mathbf{j})\exp\left[i(n+m)\phi\right]+(\mathbf{i}+i\,\mathbf{j})\exp\left[i(n-m)\phi\right]\right\},\\ \mathbf{E}_2 &= \frac{i}{2}\rho^g\left\{(\mathbf{i}-i\,\mathbf{j})\exp\left[i(n+m)\phi\right]-(\mathbf{i}+i\,\mathbf{j})\exp\left[i(n-m)\phi\right]\right\},\end{aligned} \tag{3}$$

and thus each is identified as the sum of two circularly-polarized phase singularities. Combining the two equations in Eq. (3), we obtain

#212728 - $15.00 USD Received 26 May 2014; revised 10 Jul 2014; accepted 11 Jul 2014; published 18 Jul 2014

$$\mathbf{E}_r = \mathbf{E}_1 + i\mathbf{E}_2 = \rho^g \left(\mathbf{i} + i\,\mathbf{j}\right)\exp\left[i\left(n-m\right)\phi\right],$$
$$\mathbf{E}_l = \mathbf{E}_1 - i\mathbf{E}_2 = \rho^g \left(\mathbf{i} - i\,\mathbf{j}\right)\exp\left[i\left(n+m\right)\phi\right], \tag{4}$$

giving right or left handed circularly polarized vortices. The topological charge of the phase vortex is different in the two cases. Different combinations of *n* and *m* can give the same effective result. This means that a vortex that is circularly polarized, the quadrature sum of *x* and *y* polarizations, is equivalent to the quadrature sum of, for example, radial and azimuthal polarizations with vortices of different topological charge.

3. Polarized Bessel beams

One way to generate a Bessel beam is by placing a narrow annular aperture in the front focal plane of a lens [54, 55]. If the annulus has close to a Gaussian cross-section, a Bessel-Gauss beam results. Bessel beams can be simply generalized to the non-paraxial case, i.e. they are exact solutions to Maxwell's equations. In this they differ from some other beams such as Gaussian beams. The behavior of the zero-order non-paraxial vectorial Bessel beam, as generated by focusing a plane-polarized wave, was discussed many years ago [48]. Longitudinal and cross components of polarization are introduced by focusing, so that the cross-section is broadened and divides into two spots for convergence angles greater than 65° (corresponding to a NA of 0.9 in air). Radially polarized Bessel beams (also called transverse magnetic, TM0) avoid this problem, and give a circularly-symmetric spot, with a central longitudinal polarization [13, 21, 22, 24]. Azimuthal polarization was considered by several authors [21–24]. Two further polarization distributions that give a beam with transverse linear polarization on axis are the electric dipole (ED) polarization, giving the weakest side-lobes, and the transverse electric polarization (TE1), which gives the smallest cross-section [22–24]. As the polarization produced by focusing plane-polarized light can be separated into ED and magnetic dipole (MD) parts, it has been called the mixed-dipole polarization. The mixed-dipole polarization can also be separated into TE1 and transverse magnetic (TM1) components [22–24]. TE1, TM1 and mixed-dipole polarizations are special cases of the more general spatially varying, linear polarization given in Eq. (1). ED and MD correspond to input polarizations that are inhomogeneously elliptically polarized, being circularly polarized for small θ, and azimuthally polarized as $\theta \to 90^\circ$. These can be generated by adding together different proportions, according to the value of θ, of the upper and lower solutions in Eq. (1). All of these Bessel beams are propagationally invariant in that the cross-sectional intensity does not change upon propagation, although phase and polarization state may change on propagation. In fact later we show that propagation is equivalent to a time delay.

4. Field in the focal region of a lens

We consider focusing of a wave by a lens of high numerical aperture with a narrow annular pupil. Generalizing the results of Richards and Wolf to include *y* as well as *x* polarization, the strength vector $\mathbf{e} = e_x\mathbf{i} + e_y\mathbf{j} + e_z\mathbf{k}$ on the Gaussian reference sphere of the lens can be written in terms of the incident field E_x, E_y:

$$e_x = \frac{1}{2}\left\{E_x\left[\left(1+\cos\theta\right) - \cos 2\phi\left(1-\cos\theta\right)\right] - E_y \sin 2\phi\left(1-\cos\theta\right)\right\},$$
$$e_y = -\frac{1}{2}\left\{E_x \sin 2\phi\left(1-\cos\theta\right) - E_y\left[\left(1+\cos\theta\right) + \cos 2\phi\left(1-\cos\theta\right)\right]\right\}, \tag{5}$$
$$e_z = \left(E_x\cos\phi + E_y\sin\phi\right)\sin\theta.$$

#212728 - $15.00 USD Received 26 May 2014; revised 10 Jul 2014; accepted 11 Jul 2014; published 18 Jul 2014

The terms in $\cos 2\phi$, $\sin 2\phi$ represent cross polarization, and those in $\cos\phi$, $\sin\phi$ represent longitudinal polarization. Equation (6) can be written

$$\begin{aligned} e_x &= \cos^2\frac{\theta}{2}\left[E_x\left(1-\cos 2\phi\tan^2\frac{\theta}{2}\right)-E_y\sin 2\phi\tan^2\frac{\theta}{2}\right],\\ e_y &= -\cos^2\frac{\theta}{2}\left[E_x\sin 2\phi\tan^2\frac{\theta}{2}-E_y\left(1+\cos 2\phi\tan^2\frac{\theta}{2}\right)\right],\\ e_z &= \cos^2\frac{\theta}{2}\left[\left(E_x\cos\phi+E_y\sin\phi\right)2\tan\frac{\theta}{2}\right], \end{aligned} \tag{6}$$

which shows clearly how the strength of the cross and longitudinal polarization terms increase with the angle θ, the longitudinal component increasing more rapidly. Following Richards and Wolf, the electric field at a point P (spherical coordinates r_P,θ_P,ϕ_P or cylindrical coordinates r_P,ϕ_P,z_P) in the focal region of the lens of angular semi-aperture α is

$$\mathbf{E} = -\frac{iA}{\pi}\int_0^{\alpha}\int_0^{2\pi}\mathbf{e}\cos^{1/2}\theta\exp\left(ikr_P\cos\varepsilon\right)d\phi\sin\theta d\theta \tag{7}$$

where A is a constant, $k=2\pi/\lambda$, and

$$\cos\varepsilon = \cos\theta\cos\theta_P+\sin\theta\sin\theta_P\cos\left(\phi-\phi_P\right) \tag{8}$$

with θ,ϕ the coordinates on the Gaussian reference sphere. A time variation $\exp(-i\omega t)$ has been suppressed.

We now consider what happens if the lens is illuminated with a wave that contains polarization and phase vortices. Starting from the upper case of Eq. (2), we have on the reference sphere

$$\begin{aligned} e_{x1} &= \frac{\sin^g\theta}{2}\left(\left\{\exp\left[i\left(n+m\right)\phi\right]+\exp\left[i\left(n-m\right)\phi\right]\right\}\cos^2\frac{\theta}{2}\right.\\ &\quad\left.-\left\{\exp\left[i\left(n+m-2\right)\phi\right]+\exp\left[i\left(n-m+2\right)\phi\right]\right\}\sin^2\frac{\theta}{2}\right),\\ e_{y1} &= -\frac{i\sin^g\theta}{2}\left(\left\{\exp\left[i\left(n+m\right)\phi\right]-\exp\left[i\left(n-m\right)\phi\right]\right\}\cos^2\frac{\theta}{2}\right.\\ &\quad\left.+\left\{\exp\left[i\left(n+m-2\right)\phi\right]-\exp\left[i\left(n-m+2\right)\phi\right]\right\}\sin^2\frac{\theta}{2}\right),\\ e_{z1} &= \sin^g\theta\left\{\exp\left[i\left(n+m-1\right)\phi\right]+\exp\left[i\left(n-m+1\right)\phi\right]\sin\frac{\theta}{2}\cos\frac{\theta}{2}\right\}. \end{aligned} \tag{9}$$

For the case of a Bessel beam, the integral $\sin^g\theta\cos^{1/2}\theta\sin\theta\,d\theta$ in Eq. (7) can be omitted. Then, using the identity

$$\int_0^{2\pi}\exp\left(in\phi\right)\exp\left[i\rho\cos\left(\phi-\gamma\right)\right]d\phi = 2\pi i^n J_n\left(\rho\right)\exp\left(in\gamma\right), \tag{10}$$

where $J_n(\cdot)$ is a Bessel function of the first kind, the electric field in the focal region is (after normalizing by dividing by $-2i^{n+m+1}\cos^2(\theta/2)$)

#212728 - $15.00 USD Received 26 May 2014; revised 10 Jul 2014; accepted 11 Jul 2014; published 18 Jul 2014

$$
\begin{aligned}
E_{x1} = \tfrac{1}{2}\Big(\Big\{ & J_{n+m}\left(k\rho_P \sin\theta\right)\exp[i(n+m)\phi_P] \\
& + (-1)^m J_{n-m}\left(k\rho_P \sin\theta\right)\exp[i(n-m)\phi_P]\Big\} \\
+ \tan^2\frac{\theta}{2}\Big\{ & J_{n+m-2}\left(k\rho_P \sin\theta\right)\exp[i(n+m-2)\phi_P] \\
& + (-1)^m J_{n-m+2}\left(k\rho_P \sin\theta\right)\exp[i(n-m+2)\phi_P]\Big\}\Big) \\
& \times \exp\left(ikz_P \cos\theta\right), \\
E_{y1} = -\tfrac{i}{2}\Big(\Big\{ & J_{n+m}\left(k\rho_P \sin\theta\right)\exp[i(n+m)\phi_P] \\
& - (-1)^m J_{n-m}\left(k\rho_P \sin\theta\right)\exp[i(n-m)\phi_P]\Big\} \\
- \tan^2\frac{\theta}{2}\Big\{ & J_{n+m-2}\left(k\rho_P \sin\theta\right)\exp[i(n+m-2)\phi_P] \\
& - (-1)^m J_{n-m+2}\left(k\rho_P \sin\theta\right)\exp[i(n-m+2)\phi_P]\Big\}\Big) \\
& \times \exp\left(ikz_P \cos\theta\right), \\
E_{z1} = -i\tan\frac{\theta}{2}\Big\{ & J_{n+m-1}\left(k\rho_P \sin\theta\right)\exp[i(n+m-1)\phi_P] \\
& - (-1)^m J_{n-m+1}\left(k\rho_P \sin\theta\right)\exp[i(n-m+1)\phi_P]\Big\} \\
& \times \exp\left(ikz_P \cos\theta\right). \qquad (11)
\end{aligned}
$$

The distance term combines with the time variation to give a term $\exp[i(kz_P - \omega t)]$, so that propagation is equivalent to a time delay. Similarly, for the lower case of Eq. (2), we have on the reference sphere

$$
\begin{aligned}
e_{x2} = \frac{i\sin^g\theta}{2}\Big(\Big\{ & \exp\left[i(n+m)\phi\right] - \exp\left[i(n-m)\phi\right]\Big\}\cos^2\frac{\theta}{2} \\
& - \Big\{\exp\left[i(n+m-2)\phi\right] - \exp\left[i(n-m+2)\phi\right]\Big\}\sin^2\frac{\theta}{2}\Big), \\
e_{y2} = \frac{\sin^g\theta}{2}\Big(\Big\{ & \exp\left[i(n+m)\phi\right] + \exp\left[i(n-m)\phi\right]\Big\}\cos^2\frac{\theta}{2} \qquad (12) \\
& + \Big\{\exp\left[i(n+m-2)\phi\right] + \exp\left[i(n-m+2)\phi\right]\Big\}\sin^2\frac{\theta}{2}\Big), \\
e_{z2} = i\sin^g\theta\Big\{ & \exp\left[i(n+m-1)\phi\right] + \exp\left[i(n-m+1)\phi\right]\sin\frac{\theta}{2}\cos\frac{\theta}{2}\Big\},
\end{aligned}
$$

so that in the focal region for a Bessel beam (normalizing as before)

#212728 - $15.00 USD Received 26 May 2014; revised 10 Jul 2014; accepted 11 Jul 2014; published 18 Jul 2014

$$
\begin{aligned}
E_{x2} = \tfrac{i}{2}\Big(\Big\{ & J_{n+m}\left(k\rho_P \sin\theta\right)\exp[i(n+m)\phi_P] \\
& -(-1)^m J_{n-m}\left(k\rho_P \sin\theta\right)\exp[i(n-m)\phi_P]\Big\} \\
& + \tan^2\frac{\theta}{2}\Big\{ J_{n+m-2}\left(k\rho_P \sin\theta\right)\exp[i(n+m-2)\phi_P] \\
& -(-1)^m J_{n-m+2}\left(k\rho_P \sin\theta\right)\exp[i(n-m+2)\phi_P]\Big\}\Big) \\
& \times\exp\left(ikz_P\cos\theta\right), \\
E_{y2} = \tfrac{1}{2}\Big(\Big\{ & J_{n+m}\left(k\rho_P \sin\theta\right)[i(n+m)\phi_P] \\
& +(-1)^m J_{n-m}\left(k\rho_P \sin\theta\right)\exp[i(n-m)\phi_P]\Big\} \\
& - \tan^2\frac{\theta}{2}\Big\{ J_{n+m-2}\left(k\rho_P \sin\theta\right)[i(n+m-2)\phi_P] \\
& +(-1)^m J_{n-m+2}\left(k\rho_P \sin\theta\right)[i(n-m+2)\phi_P]\Big\}\Big) \\
& \times\exp\left(ikz_P\cos\theta\right), \\
E_{z2} = \tan\frac{\theta}{2}\Big\{ & J_{n+m-1}\left(k\rho_P \sin\theta\right)\exp[i(n+m-1)\phi_P] \\
& +(-1)^m J_{n-m+1}\left(k\rho_P \sin\theta\right)\exp[i(n-m+1)\phi_P]\Big\} \\
& \times\exp\left(ikz_P\cos\theta\right). \qquad (13)
\end{aligned}
$$

For the case of a paraxial beam, we can put θ as small, giving for the first solution

$$
\begin{aligned}
E_{x1} = \tfrac{1}{2}\Big\{ & J_{n+m}\left(k\rho_P \sin\theta\right)\exp[i(n+m)\phi_P] \\
& +(-1)^m J_{n-m}\left(k\rho_P \sin\theta\right)\exp[i(n-m)\phi_P]\Big\}\exp\left(ikz_P\cos\theta\right), \\
E_{y1} = -\tfrac{i}{2}\Big\{ & J_{n+m}\left(k\rho_P \sin\theta\right)\exp[i(n+m)\phi_P] \\
& -(-1)^m J_{n-m}\left(k\rho_P \sin\theta\right)\exp[i(n-m)\phi_P]\Big\}\exp\left(ikz_P\cos\theta\right). \qquad (14)
\end{aligned}
$$

There is no longitudinal field component. For the second solution

$$
\begin{aligned}
E_{x2} = \tfrac{i}{2}\Big\{ & J_{n+m}\left(k\rho_P \sin\theta\right)\exp[i(n+m)\phi_P] \\
& -(-1)^m J_{n-m}\left(k\rho_P \sin\theta\right)\exp[i(n-m)\phi_P]\Big\}\exp\left(ikz_P\cos\theta\right), \\
E_{y2} = \tfrac{1}{2}\Big\{ & J_{n+m}\left(k\rho_P \sin\theta\right)\exp[i(n+m)\phi_P] \\
& +(-1)^m J_{n-m}\left(k\rho_P \sin\theta\right)\exp[i(n-m)\phi_P]\Big\}\exp\left(ikz_P\cos\theta\right). \qquad (15)
\end{aligned}
$$

Equations (11) and (13)–(15) can be applied to different combinations of phase and polarization vortices. We make the following general observation. As the Bessel function has a non-zero value for zero argument for order zero, for the paraxial case there is a non-zero field on axis only if $n+m=0$ or $n-m=0$. These cases include the special cases $n=m=0$, when there are no vortices; $m=1, n=\pm1$ corresponding to radial and azimuthal polarization with a phase vortex for cases 1 (Eq. (14)) and 2 (Eq. (15)), respectively [21–24]; $m=-1, n=\pm1$ corresponding to a parallel screw disclination with a phase vortex; and $m=2, n=\pm2$ corresponding to a dipole dislocation with a charge two phase vortex. One of the conditions is also satisfied by the fractional indices $m=-1/2, n=\pm1/2$ and $m=1/2, n=\pm1/2$. These are related to the star and lemon singularities. Although other non-

#212728 - $15.00 USD Received 26 May 2014; revised 10 Jul 2014; accepted 11 Jul 2014; published 18 Jul 2014

integer values of m,n may satisfy one of the conditions, the half-integer values are special because a rotation of direction by π is equivalent to a phase change of π, and hence there is no discontinuity of phase.

Turning to the non-paraxial case, we see from Eqs. (11) and (13) that there is a longitudinal field component on the axis of order $\tan(\theta/2)$ if $n+m-1=0$ or $n-m+1=0$. Although this is weak for small θ, in systems of high NA it can become strong. Examples are $m=-1,n=\pm 2$, $m=0,n=\pm 1$, $m=1,n=0$, $m=2,n=\pm 1$. For a plane-polarized phase vortex of unit charge, the zero of the vortex is filled in by the longitudinal field component. It should be noted that on the axis there is a z component of field only, so that this component has a well-defined phase, and the wave is linearly polarized in the direction of propagation. The axis is thus an L^T line [27]. Here the superscript T refers to 'true', i.e. three dimensional. For radially polarized illumination with no phase vortex there is also a longitudinal field component. However, for azimuthal polarization, the two parts of the E_z term in Eq. (13) cancel. Interestingly, for the vortex $m=n=1/2$, there is also a longitudinal field component on axis, in addition to the transverse component.

There is also a transverse axial field component of order $\tan^2(\theta/2)$ if $n+m-2=0$ or $n-m+2=0$. Examples are $m=-1,n=\pm 3$, $m=0,n=\pm 2$, $m=1,n=\pm 1$, $m=2,n=0$. For a plane-polarized phase vortex of charge two, the zero of the vortex is filled in by the transverse cross-field component. The field on the axis is thus again nonzero, and is transverse and right hand circularly polarized, even though the illumination is plane polarized. The axis is a C^T line [27]. For a dipole polarization vortex with no phase vortex there is also a transverse field on axis.

For $m=0$ and values of $|n|\geq 3$, or for $n=0$ and $m\geq 3$ or $m\leq -1$, there is a zero in intensity on the axis as all components exhibit zeros on axis. Near to the axis, the field is predominantly transverse and circularly polarized. For $n=0,m=-1$, corresponding to parallel screw disclination, the field is thus zero on axis. For low NAs, the J_1 terms dominate, and the intensity is axially symmetric. As θ increases, the relative strength of the axial field component increases, which introduces an intensity component with four-fold rotational-symmetry.

For $n=0,m=2$, corresponding to a dipole polarization vortex, for low NAs, the J_2 terms dominate, and the intensity is zero on axis and exhibits four-fold rotational-symmetry. As θ increases, the other components increase in strength. The intensity exhibits two-fold symmetry, with the field linearly polarized in the transverse direction on axis. Plots of the intensity variation were given by Sheppard [48].

5. Circular polarized phase singularity

Equation (3) showed that the combined phase and polarization vortices can be considered as the sum of two circularly-polarized phase vortices. From Eq. (4), we see that the field depends only on $n\mp m$ for right/left circular polarization, respectively, which we take as p in each case. For the case of a circularly polarized phase vortex, the field in the back focal plane is thus taken to be

$$\begin{aligned}\mathbf{E}_r &= \mathbf{E}_1 + i\mathbf{E}_2 = \rho^g\left(\mathbf{i}+i\,\mathbf{j}\right)\exp(ip\phi),\\ \mathbf{E}_l &= \mathbf{E}_1 - i\mathbf{E}_2 = \rho^g\left(\mathbf{i}-i\,\mathbf{j}\right)\exp(ip\phi).\end{aligned} \tag{16}$$

Then on the reference sphere

#212728 - $15.00 USD Received 26 May 2014; revised 10 Jul 2014; accepted 11 Jul 2014; published 18 Jul 2014

$$
\begin{aligned}
e_x &= \sin^g\theta\cos^2\frac{\theta}{2}\exp(ip\phi)\left\{1-\exp(\pm i2\phi)\tan^2\frac{\theta}{2}\right\},\\
e_y &= \pm i\sin^g\theta\cos^2\frac{\theta}{2}\exp(ip\phi)\left\{1+\exp(\pm i2\phi)\tan^2\frac{\theta}{2}\right\},\\
e_z &= 2\sin^g\theta\cos^2\frac{\theta}{2}\exp(ip\phi)\exp(\pm i\phi)\tan\frac{\theta}{2}.
\end{aligned}
\tag{17}
$$

Neglecting a constant multiplier, we obtain for the field in the focal region for a circularly-polarized Bessel beam

$$
\begin{aligned}
E_x &= \Big\{J_p\left(k\rho_P\sin\theta\right)\exp(ip\phi_P)\\
&\qquad +\tan^2\frac{\theta}{2}J_{p\pm2}\left(k\rho_P\sin\theta\right)\exp[i(p\pm2)\phi_P]\Big\}\exp\left(ikz_P\cos\theta\right),\\
E_y &= \pm i\Big\{J_p\left(k\rho_P\sin\theta\right)\exp(ip\phi_P)\\
&\qquad -\tan^2\frac{\theta}{2}\left\{J_{p\pm2}\left(k\rho_P\sin\theta\right)\exp[i(p\pm2)\phi_P]\right\}\Big\}\exp\left(ikz_P\cos\theta\right),\\
E_z &= \pm i2\tan\frac{\theta}{2}J_{p\pm1}\left(k\rho_P\sin\theta\right)\exp[i(p\pm1)\phi_P]\exp\left(ikz_P\cos\theta\right).
\end{aligned}
\tag{18}
$$

For the paraxial case, this reduces to

$$
\begin{aligned}
E_x &= J_p\left(k\rho_P\sin\theta\right)\exp(ip\phi_P)\exp\left(ikz_P\cos\theta\right),\\
E_y &= \pm i\,J_p\left(k\rho_P\sin\theta\right)\exp(ip\phi_P)\exp\left(ikz_P\cos\theta\right),
\end{aligned}
\tag{19}
$$

as we might expect. From Eq. (17), for $p=1$ for the first solution, and $p=-1$ for the second solution, all the field components are zero on axis, and we obtain a true phase singularity, corresponding to a circularly polarized beam with a unity charge phase vortex. Note that as a plane-polarized beam with a phase vortex was shown not to exhibit a zero on axis, the zero for the circular polarization case depends critically on the polarization being exactly circular. This is important for applications in stimulated emission depletion (STED) microscopy [41, 42]. For $p=-1$ for the first solution or $p=1$ for the second solution, there is a longitudinal field component on axis. This corresponds to the case when the handedness of the phase vortex is in the opposite sense to that of the circular polarization. Similarly, for $p=2$ for the first solution, or for $p=-2$ for the second solution there is a true phase singularity, while for $p=-2$ for the first solution, or $p=2$ for the second solution, there is a transverse, circularly polarized, field on axis.

6. Half-order phase vortices

We now investigate the behavior of fractional order vortices $m=\pm1/2, n=1/2$, which produce an intensity maximum on axis. The results shown are for the upper solution in Eq. (1). The lower solution is just rotated, while $n=-1/2$ produces rotations with time in the opposite direction. First we examine the case of a paraxial Bessel beam. The behavior is plotted against normalized optical coordinates $v_x=kx\sin\theta, v_y=ky\sin\theta$. Figures 3 and 5 show the Stokes parameters for the cases $m=\pm1/2, n=1/2$, respectively. Stokes' parameter S_0, which represents the intensity of the beam, is axially symmetric, and the same in both cases. The cross-section is shown in Fig. 4. S_1, S_2 give the linearly polarized components. S_3 gives the circularly polarized component, which is also axially symmetric, with opposite

#212728 - $15.00 USD Received 26 May 2014; revised 10 Jul 2014; accepted 11 Jul 2014; published 18 Jul 2014

handedness for the two cases. S_1, S_2, S_3 are plotted in the range $[-1,1]$. On the axis, the beam is fully circularly polarized. At $v = 1.43$, then again at $v = 3.12$, $S_3 = 0$, and the beam is linearly polarized. Interestingly, these are both inside the central lobe of the Airy disc, so if the circularly polarized component were separated, it would be much narrower than the Airy disc (about half the width). In Figs. 3 and 5 we also show various parameters of the polarization ellipse. The orientation angle ψ is given by $\tan 2\psi = S_2 / S_1$. The ellipticity χ is given by $\sin 2\chi = S_3 / S_0$. The auxiliary angle α is given by $\cos 2\alpha = S_1 / S_0$. The phase δ difference is given by $\tan \delta = S_3 / S_2$. ψ is plotted in the range $[-\pi/2, \pi/2]$ in steps of $\pi/10$, from dark to light. χ is plotted in the range $[-\pi/4, \pi/4]$ in steps of $\pi/20$. α is plotted in the range $[0, \pi/2]$ in steps of $\pi/20$. δ is plotted in the range $[-\pi, \pi]$ in steps of $\pi/5$. None of these quantities depend on the absolute phase. The angle δ' is the phase along the major axis of the polarization ellipse. In each lobe, there is a phase change of π on making a circuit counter-clockwise around the axis.

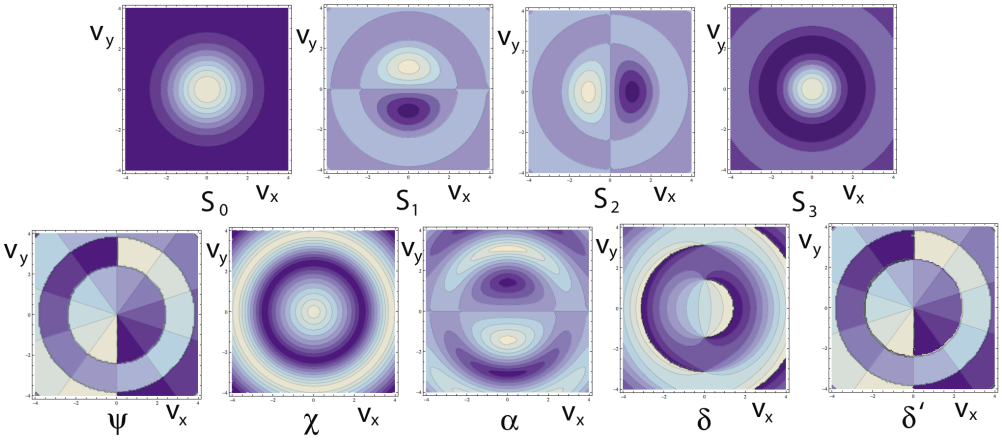

Fig. 3. Parameters for the case $m = 1/2, n = 1/2$. The top row shows the Stokes parameters. The bottom row show $\psi, \chi, \alpha, \delta, \delta'$.

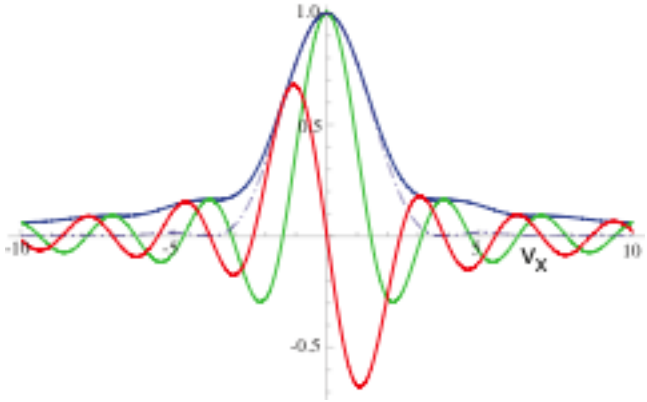

Fig. 4. A cross section through the beam at $y = 0$ for $m = 1/2, n = 1/2$. S_0 is shown in blue, S_2 in red, and S_3 in green. The Airy disc is shown as a chained line for comparison.

#212728 - $15.00 USD Received 26 May 2014; revised 10 Jul 2014; accepted 11 Jul 2014; published 18 Jul 2014

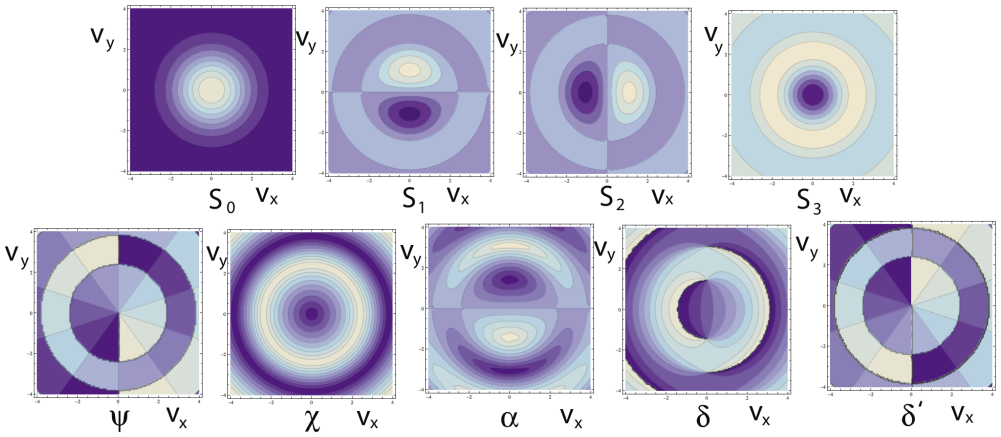

Fig. 5. Parameters for the case $m=-1/2, n=1/2$. The top row shows the Stokes parameters. The bottom row show $\psi, \chi, \alpha, \delta, \delta'$.

The time-variation of the polarization is illustrated in Fig. 6(a), Media 3, and Fig. 6(b), Media 4, which show the vector field of the beam for $m=\pm 1/2$, respectively. In Fig. 6(a), Media 3, a polarization vortex near to the axis rotates around in a circle, changing continuously from radial to azimuthal polarization and so on. In Fig. 6(b), Media 4, the polarization vortex near to the axis is a parallel screw disclination, which rotates as the vortex rotates. In three dimensions, the vortex spirals around the axis as the beam propagates.

As the angular aperture of the beam increases, the other polarization terms become significant. Although the intensity of the beams is the same for $m=\pm 1/2$ in the paraxial case, for large convergence angles they become different, as shown in Fig. 7. For $m=1/2, n=1/2$ there is a longitudinal field component on the axis, in addition to the circularly polarized transverse field. At the origin, the electric field vector is $\{i[\mathbf{i}-2\tan(\theta/2)\mathbf{k}]-\mathbf{j}\}/2$, so that the field is elliptically polarized in a plane tilted at an angle $\arctan[2\tan(\theta/2)]$. For $m=-1/2, n=1/2$ the longitudinal component has terms with J_1 and J_2, which increase the width of the beam. By $\theta=75^\circ$, the maximum intensity is no longer on the axis. For the non-paraxial case, the polarization and vectorial behaviors are rather complicated, and we do not discuss them here.

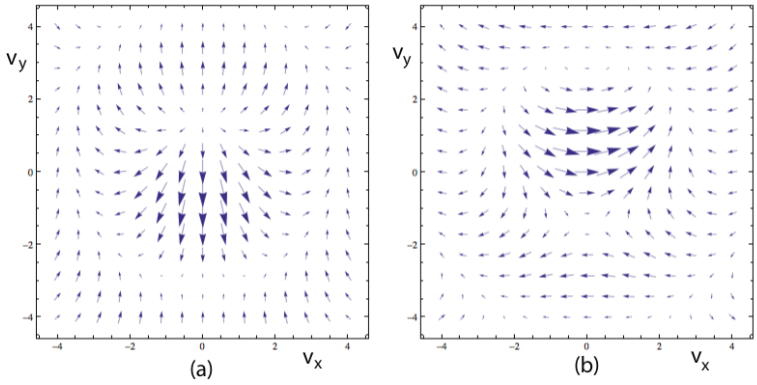

Fig. 6. The vector electric field of Bessel beams at time $t=0$, with the time variation shown in the media, for (a) $m=1/2, n=1/2$ (Media 3), and (b) $m=-1/2, n=1/2$ (Media 4).

#212728 - $15.00 USD Received 26 May 2014; revised 10 Jul 2014; accepted 11 Jul 2014; published 18 Jul 2014

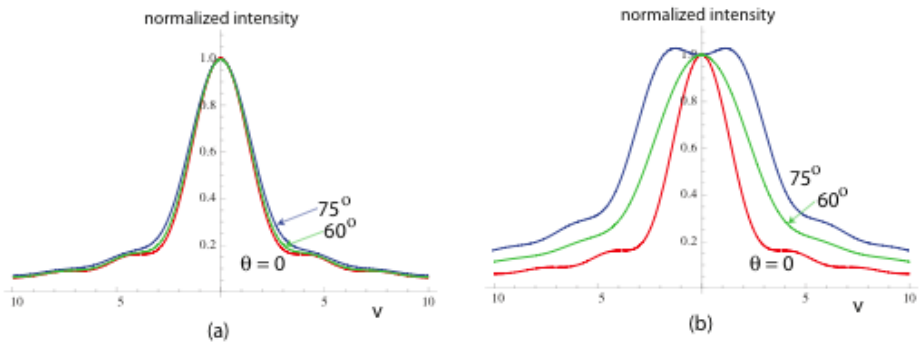

Fig. 7. The intensity of a non-paraxial Bessel beam of semi-angle of convergence $\theta = 0, 60^{\circ}, 75^{\circ}$, for (a) $m = 1/2, n = 1/2$, and (b) $m = -1/2, n = 1/2$.

7. Discussion

The focusing of beams exhibiting both phase vortices and polarization vortices, by an aplanatic lens of high NA, has been analysed. Equations are given for the electric field of Bessel beams with different polarization and phase vortex conditions. These can be integrated to calculate the focused field of a lens of high NA.

If a linearly polarized beam including a phase vortex of unity charge is focused by a high NA lens, there is an axial electric field component on the axis. For a phase vortex of charge two there is a weak transverse field on axis. Thus in both these cases, there is not strictly a phase singularity in the focused field. For $n \geq 3$, there is a zero in electric field on the axis. Circularly polarized beams with a phase vortex can result in a zero axial field component, but only for the correct handedness of the vortex. Polarization vortices can exhibit TE or TM behavior (order $m = 1$). Beams with a polarization vortex of order $m = -1$ result in a zero in electric field on the axis after focusing. Beams with a polarization vortex of order $m = 2$ when focused have a transverse, linearly polarized electric field on axis. Beams exhibiting a combination of polarization and phase vortices can be decomposed into a summation of circularly polarized beams, each in general with phase vortices. A TE beam $n = m = 1$ gives a focused spot with a bright centre and, obviously, no axial electric field component. A TM beam $n = m = 1$ also gives a focused spot with a bright centre. Combinations of n and m that are half-integer give novel, physically realizable, polarized Bessel beams.

Acknowledgments

The author thanks Eileen Sheppard for checking the algebra, and Shalin Mehta for assistance with the multimedia.

#212728 - $15.00 USD Received 26 May 2014; revised 10 Jul 2014; accepted 11 Jul 2014; published 18 Jul 2014